Defraeye T., Lambrecht R., Delele M.A., Ambaw A., Opara U.L., Cronjé P., Verboven P., Nicolai B. (2014), Forced-convective cooling of citrus fruit: cooling conditions and energy consumption in relation to package design, *Journal of Food Engineering* 121, 118-127. http://dx.doi.org/10.1016/j.jfoodeng.2013.08.021

Forced-convective cooling of citrus fruit: cooling conditions and energy consumption in relation to package design

Thijs Defraeye [a, *], Rutger Lambrecht [a], Mulugeta Admasu Delele [c], Alemayehu Ambaw Tsige [a], Umezuruike Linus Opara [c], Paul Cronjé [d], Pieter Verboven [a], Bart Nicolai [a,b]

[a] *MeBioS, Department of Biosystems, University of Leuven, Willem de Croylaan 42, 3001 Heverlee, Belgium*

[b] *VCBT, Flanders Centre of Postharvest Technology, Willem de Croylaan 42, 3001 Heverlee, Belgium*

[c] *South African Research Chair in Postharvest Technology, Stellenbosch University, Stellenbosch 7602, South Africa*

[d] *Citrus Research International, Department of Horticultural Sciences, Stellenbosch University, Stellenbosch 7602, South Africa*

[*] Corresponding author. Tel.: +32 (0)16321618; fax: +32 (0)16322966.
E-mail address: thijs.defraeye@biw.kuleuven.be

Defraeye T., Lambrecht R., Delele M.A., Ambaw A., Opara U.L., Cronjé P., Verboven P., Nicolai B. (2014), Forced-convective cooling of citrus fruit: cooling conditions and energy consumption in relation to package design, *Journal of Food Engineering* 121, 118-127. http://dx.doi.org/10.1016/j.jfoodeng.2013.08.021

Abstract

The performance of an existing container for orange fruit and two new designs, stacked on a pallet, has been evaluated for forced-convective precooling using computational fluid dynamics. The focus was on the fruit cooling rate and the system energy consumption in relation to cooling conditions (airflow rate and cooling temperature). The new package designs both showed an improved cooling rate and cooling uniformity, although this improvement is to some extent dependent on the cooling system that is used, which should also be taken into account when evaluating package design. The energy required to maintain airflow through the containers during the precooling process was also less for the new containers due to their lower aerodynamic resistance. These new containers seem a cost-effective way for improving forced-convective precooling of orange fruit with respect to throughput, fruit quality and operational cost of the system. In this study, basic information on the containers was obtained to guide future cold-chain design decisions and changes to existing cooling protocols or cooling systems.

Keywords

computational fluid dynamics; convective transfer; precooling; cold chain; operational cost; cold sterilisation

1. Introduction

Forced-convective precooling of horticultural produce after harvest, to remove the field heat, is a critical step in the food cold chain since the postharvest food quality, storage time and shelf life are strongly related to the product temperature. Though it is the most widely used precooling method (Dehghannya et al., 2010), there is still a large potential for optimisation, both with respect to product quality as well as the cooling system. This implies reduced operational (energy) costs, increased throughput, an increased product lifetime and lower food losses. Such cold-chain optimisation challenges will become crucial in the coming decades due to the growing need for food (projected to grow with 70% by 2050; FAO, 2009) and for reducing energy consumption to produce and process food.

Product quality should be optimised by providing fast cooling without introducing chilling injury (Thompson, 2003), as well as uniform cooling of individual products to ensure uniform quality (Dehghannya et al., 2010; Nahor et al., 2005). Cooling system optimisation involves, amongst others, determining the optimal working point of the system (i.e., the required flow rate) that minimises the cooling time of the food, thus maximises throughput, and limits operational costs in the system, thus its energy consumption.

The cooling rate and uniformity of horticultural produce depend on their size, shape and thermal properties but also on airflow rate, cooling temperature and accessibility of the cooling air to the produce. The latter is determined by the product stacking in the containers, the design of the container (location of vent holes and total vent area; Pathare et al., 2012; van der Sman, 2002) but also by the stacking of individual containers on a pallet, as vent holes might be closed after palletisation or the airflow can bypass the produce through openings between individual containers (Defraeye et al., 2013; Ferrua and Singh, 2009). Apart from their impact on the cooling rate, these properties of produce and containers are closely linked to the operational costs of the system since a significant amount of energy is consumed by the fans to maintain airflow through the stacks of containers during the cooling process, in addition to the energy required for cooling the air. Here, the required fan power is largely determined by the aerodynamic resistance of the stack and the containers. Hence, cooling conditions, packaging and palletisation play a key role in the cooling rate, throughput and energy consumption of the forced-convective precooling process.

Containers of horticultural produce are, however, often designed and optimised with the focus on mechanical strength, instead of cooling performance or reduction of the airflow resistance, by which often product quality, throughput and operational costs can still be improved. Apart from experiments, integrated package performance analysis can be done using numerical techniques, such as computational fluid dynamics (CFD, see Defraeye et al., 2013; Dehghannya et al., 2011, 2012; Delele et al., 2012; Ferrua and Singh, 2009; Pathare et al., 2012; Verboven et al., 2006; Zou et al., 2006a, 2006b), which is often less cost- and labour-intensive (e.g., Defraeye et al., 2013). This tool allows to obtain the airflow characteristics and pressure losses of packaging and pallets as well as information on the cooling performance at a high spatial and temporal resolution (Dehghannya et al., 2010; Smale et al., 2006).

The focus of this study is on forced-convective precooling of oranges, which account for more than half of the global citrus fruit produced and which showed an increase in production of 70% compared to 1980 (FAOSTAT, 2012). This research was mainly conducted for the South-African citrus industry, which is currently the third largest citrus exporter worldwide, within the framework of their cold sterilisation treatment. This phytosanitary treatment includes several weeks of storage at a sub-zero temperature (≈ -0.5°C). It is requested by some export markets (currently below 10% of the South-African markets) to prevent the infection by false codling moth, which is a typical pest for South-Africa. Since the oranges have to be precooled to lower temperatures (for normal precooling ≈ 2-4°C, e.g., Thompson, 2003), the precooling time increases and the achievable throughput is reduced. More markets are expected to ask this treatment, which will put severe pressure on the South-African postharvest industry, as maintaining the same throughput will not be possible with the current cooling systems. Adjusting or increasing the precooling capacity is however not straightforward nor economically beneficial. Therefore the development of new container designs was explored as a cost-effective alternative to increase throughput for the currently installed cooling capacity.

CFD is used in this study to evaluate the performance of three container designs, namely an existing corrugated fibreboard container (CFC) and two new container designs, namely the Supervent CFC and the Ecopack reusable plastic container (RPC). The aim is to calculate the influence of cooling conditions (airflow rate, cooling temperature) on the cooling rate of oranges, packed in containers which are stacked on a pallet, and on the energy consumption (operational cost) of the system. The outcome is to gain insight in the cooling rate and energy consumption of the three container designs and to provide basic information to guide changes to existing cooling protocols or cooling systems. This study is a follow-up of Defraeye et al. (2013), which evaluated the performance of CFD for these three container designs by comparison with experiments at a single flow rate and cooling temperature.

2. Materials and methods

2.1 Package types

Two types of telescopic CFC's were evaluated (see Figure 1). The only difference between the two CFC's is the number, size and positioning of the different vent holes: the standard container, with a conservative design, has two circular vents on each side, at half height; the Supervent container has half-circular vent holes, located at the top and bottom of each side. A (horizontal) ventilation pathway is formed via these vent holes, when several containers are stacked on a pallet. As forced-convective precooling is achieved here by horizontal airflow, the impact of the horizontal openings on the bottom and top of the containers on the cooling process is assumed negligible.

The third type of container was a reusable plastic container called Ecopack (see Figure 1). The fruit is kept in position by means of a net and a plastic foil. For this container, horizontal flow should always be perpendicular to the long side as the short side is almost completely blocked by the plastic foil. Table 1 summarises the total open area (TOA) of the sides for both CFC types and for the Ecopack RPC.

2.2 Numerical model

Numerical models were constructed to study horizontal flow through these three types of containers, as stacked on a pallet. These models are shown in Figure 2 with the dimensions and boundary conditions. Standard and Supervent containers are typically stacked in three rows on a pallet, with the most downstream row perpendicular to the other two. Some simplifications were made compared to reality to limit the computational cost, amongst others: (i) Only one layer of containers (Figure 2) was modelled for both CFC's and only two layers for the RPC, namely the layer(s) in the middle, by assuming symmetry on top and bottom boundaries; (ii) The Ecopack container geometry was simplified, by which the total open area was slightly higher, namely 62% (Table 1); (iii) The plastic net was not included for Ecopack due to its high porosity and the plastic foil was also not modelled as it was parallel to the (horizontal) airflow direction, which was found to be a reasonable assumption since flow inside the stack was predominantly horizontal (results not shown). Individual oranges were modelled discretely as spheres with a diameter of 80 mm. Each container held 64 (CFC's) or 80 oranges (Ecopack) and was filled according to a staggered pattern. Since 10 containers were modelled for the CFC's and 8 containers for Ecopack, the amount of oranges in all computational models was equal, namely 640 oranges. Although the container footprint of the CFC's is different from that of Ecopack, the volumetric packing density of the oranges in the containers is about the same for both types of containers since their height also differs (*z*-direction in Figure 2). The upstream and downstream sections of the computational domain were taken sufficiently long to avoid an influence of inlet and outlet boundary conditions on the flow in the proximity of the containers.

The computational grid was a hybrid grid (hexahedral and tetrahedral cells) with 5.5×10^6, 5.4×10^6 and 5.5×10^6 cells for standard, Supervent and Ecopack containers, respectively. The spatial discretisation error was estimated by means of Richardson extrapolation (Franke et al., 2007; Roache, 1994) and was about 2.5% for the mass flow rate through the containers and 5% for the heat flow from the oranges.

At the inlet of the domain, the ambient atmospheric pressure was imposed, i.e., the conditions in a normal cool room. A low turbulence intensity (0.05%) was imposed for flow entering the computational domain, similar to Defraeye et al. (2013). The inlet air temperature was taken representative for cooling conditions used in the South-African citrus industry for cold sterilisation treatment, namely -0.5°C, but in some simulations (see sections 3.1.3 and 3.2.3) a higher (i.e., normal) set temperature was also evaluated (4°C).

At the outlet, an underpressure was imposed, as induced by the fans in the cooling system. Different underpressures were evaluated to investigate the effect of airflow rate on cooling rate: 100 Pa, 1000 Pa and 10000 Pa for standard and Supervent containers; 10 Pa, 100 Pa and 1000 Pa for the Ecopack container, which were taken lower due to its lower airflow resistance. These pressures were chosen in order to obtain airflow rates in the simulations that are realistic for industrial forced-convective precooling. The corresponding flow rates (in L $s^{-1}kg^{-1}$ of fruit), average air speed at the inlet of the computational domain and resulting average superficial air speed inside the fruit stacks in the containers are given in Table 2. The resulting flow rate range is realistic for forced-convective precooling in industry: typical flow rates of 1 to 3 L $s^{-1}kg^{-1}$ of fruit have been reported (Brosnan and Sun, 2001). The magnitude of the flow rates also agrees well with the experiments performed by Defraeye et al. (2013).

The bottom and top surfaces and the lateral boundaries upstream and downstream of the containers were modelled as symmetry boundary conditions (slip walls), which assume that the normal velocity component and the normal gradients at the boundary are zero. The cardboard and plastic containers and the fruit surfaces were modelled as no-slip walls with zero roughness. At the sides of the containers, the heat exchange with the cool room (i.e. the heat flux) was modelled (calculated) by means of a convective heat transfer coefficient (CHTC [W $m^{-2}K^{-1}$], taken equal to 8 W $m^{-2}K^{-1}$, which is representative for indoor conditions) and the room temperature. The CHTC relates the convective heat flux normal to the surface ($q_{c,w}$ [J $s^{-1}m^{-2}$]), i.e., at the air-material interface, to the difference between the wall temperature (T_w [°C or K]) and a reference temperature (T_{ref} [°C or K]), which was the cool room temperature in this study: CHTC = $q_{c,w}/(T_w-T_{ref})$. The flux is assumed positive away from the surface. The initial temperature of the fruit and cardboard/plastic was taken equal to the characteristic fruit temperature after being packed and palletised, which was typically 20°C for South Africa.

2.3 Numerical simulation

In the past, CFD has been extensively applied to model fluid flow for several food processing applications (Ambaw et al., 2012; Delele et al., 2008, 2012; Hu and Sun, 2001; Verboven et al., 2003; Zou et al., 2006a, 2006b). The accuracy of CFD simulations depends to a large extent on the turbulence-modelling and boundary-layer modelling approaches that are used. In this study, Reynolds-averaged Navier-Stokes (RANS) in combination with the shear stress transport k-ω model (SST k-ω; Menter, 1994) was applied. It was not feasible to mesh the boundary-layer region fine enough to apply low-Reynolds number modelling to resolve the flow in the boundary layer on the no-slip surfaces (e.g., fruit) since the computational cost would be too large and grid generation is very challenging for the configuration under study. Therefore, the wall-function approach was used. Despite being less accurate (e.g., Defraeye et al., 2010), wall functions are often the only option as low-Reynolds number modelling is not practically applicable for complex 3-D configurations (Defraeye et al., 2012; Kondjoyan, 2006).

This RANS turbulence model in combination with wall functions was applied in a related study on cooling of orange fruit (Defraeye et al., 2013) with a very similar configuration (as in Figure 2). The satisfactory agreement with experimental data indicated a sufficient accuracy of the CFD simulations. Other studies using this turbulence model with wall functions also found a good agreement with experiments (Ambaw et al., 2012; Delele et al., 2009).

The simulations were performed with the CFD code ANSYS Fluent 13. Second-order discretisation schemes were used throughout. The SIMPLE algorithm was used for pressure-velocity coupling. Pressure interpolation was second order. Buoyancy effects were considered negligible and were not taken into account in the simulations, which implies forced-convective flow and passive scalar (heat) transfer. Radiation was also not considered in the simulations since the radiation exchange between the fruit inside the stack was considered small compared to convective heat transfer. Heat of respiration was not included in the model since it is unlikely to have a significant impact on the cooling rate of fresh horticultural produce during forced-convective precooling (Brosnan and Sun, 2001; Gowda et al., 1997) and it is quite low for oranges (~ 50 W $tonne^{-1}$; ASHRAE, 1994). Mass loss from the fruit and the resulting latent heat of evaporation were also not included in the model since the mass loss was very small (measured as < 1% after 3 days at -0.5°C, of which one day with airflow, results not reported). Iterative convergence of the numerical simulation was assessed by monitoring the velocity, turbulent kinetic energy and temperature at specific locations in the flow field, and the heat fluxes (surface-averaged values) on the fruit surfaces. Following thermal properties of the oranges were used in the simulations: a density of 960 kg m^{-3}, a thermal conductivity of 0.386 W $m^{-1}K^{-1}$ and a specific heat capacity of 3850 J $kg^{-1}K^{-1}$ (ASHRAE, 1993). These properties were taken constant, thus independent of temperature.

Before simulating the transient cooling process, steady-state simulations were performed to obtain the flow field and the initial temperature conditions. During these simulations, the temperatures of the containers and fruit were fixed to their initial value (20°C) and the inlet temperature was taken equal to the cool room temperature (-0.5°C or 4°C). After the steady-state simulations, transient simulations of the precooling process were performed. Since the flow field was steady over time, amongst others since no buoyancy was included in the model, the flow field did not need to be resolved anymore during the transient simulations and thus the flow equations were switched off. As such, the computational cost was reduced since only the energy equation needed to be solved. The transient simulations were run for 20h, with a time step of 60s, which was determined from temporal sensitivity analysis. The simulation of the standard container at 100Pa was run for 40h, due to its low cooling rate. The simulations (for 20h) took roughly 35h on a 12 core Intel Xeon processor (2.66GHz) with 48GB RAM memory.

2.4 Evaluation of cooling rate

The cooling rate of each container was assessed by monitoring the temperature in the centre of a single orange, located in the central part of the container, which acts as a virtual sensor. From these temperature profiles, the fractional unaccomplished temperature change (Y) could be determined:

$$Y = \frac{T - T_a}{T_i - T_a} \tag{1}$$

where subscripts i and a represent the initial temperature of the fruit (20°C) and the set cooling air temperature (-0.5°C or 4°C), respectively. The half cooling time (HCT, $t_{1/2}$) and the seven-eighths cooling time (SECT, $t_{7/8}$) are the times required to reduce the temperature difference between the fruit and the cooling air by half (Y = 0.5) or seven eighths (Y = 0.125). The SECT is particularly interesting in commercial cooling operations because the fruit temperature is then acceptably close to the required storage temperature. At this point, the fruit can be shipped or transferred to storage facilities where the remaining heat load can be removed with less energy costs (Brosnan and Sun, 2001). In addition to these parameters, the CHTC at the surface of the oranges was also determined in the same way as described in section 2.2: CHTC = $q_{c,w}/(T_w-T_{ref})$, with $q_{c,w}$ the convective heat flux at the air-material interface, T_w the surface temperature at the start of the simulations (i.e. the initial fruit temperature, 20°C), which was thus uniform, and T_{ref} the (inlet) temperature of the cool room (-0.5°C or 4°C). As this temperature difference (T_w-T_{ref}) was constant over all fruit surfaces when calculating the CHTC, the CHTC is actually directly proportional to the heat flux at the wall ($q_{c,w}$). Note that other reference temperatures can also be taken to define the CHTC, such as the bulk air temperature at the inlet of each row or even of each individual container. In this study, preference was given to use a single reference temperature to define the CHTC for the entire system of containers, i.e. that at the inlet, which can also be easily measured in experiments. The CHTC is a simplified and straightforward parameter for representing and quantifying heat flows in complex heat transfer problems. Users of such CHTC information should however verify that they apply the appropriate reference temperature, i.e. the one which was used to define the CHTC.

2.5 Evaluation of system energy consumption

In precooling systems, the energy consumption is mainly determined by: (1) the field heat stored in the oranges; (2) the energy consumption of the ventilation system (fans) which maintains airflow through the stack of containers; (3) the efficiency of the cooling unit (COP); (4) the heat produced by respiration; (5) the heat losses from the refrigerator room to the outside environment; (6) air infiltration; (7) the moisture evaporation from the fruit. For precooling systems which are properly designed (i.e. well-insulated and a small amount of leakage), the first three contributions are usually the most significant.

When comparing different package designs, the field heat to be removed is the same for all package designs as all packages contain in total the same amount of fruit and as the thermal mass of the containers themselves was negligible (below 1.5% of that of the fruit). As such, a possible reduction in energy consumption lies mainly in the ventilation system and is determined by the power required to produce airflow (i.e., fan power) and the time needed to maintain this airflow (i.e., cooling time). Both are closely related to the package design: the aerodynamic resistance of the containers stacked on a pallet (pressure drop) determines the required fan power and the working point of the system (intersection of fan performance curve and system curve); the vent hole configuration and total open area determines the cooling time (e.g., SECT).

An estimate of the energy consumption of the different container designs for fruit precooling (in Joule) was made by multiplying the power required (in Watt) to force air through the computational model of the containers (single layer for CFC's and two layers for Ecopack, all containing in total the same amount of fruit, see Figure 2) with the required precooling time, for which the SECT (s) was taken. Note that the resulting amount of energy only includes the contribution of the packages (one or two layers), whereas the total operational cost also includes contributions of other components of the ventilation system (e.g., see de Castro et al., 2005). Although this energy estimate is only an indicative value, it allows relative comparison of container designs.

The power (P_w) required to force air through the computational model (one or two layers of containers) was calculated as the product of the pressure drop over the layer (ΔP, Pa) and the flow rate through the computational domain (G_a, m³ s^{-1}):

$$P_w = \Delta P G_a \qquad (2)$$

This pressure drop equals:

$$\Delta P = \xi_1 G_a^2 + \xi_2 G_a \qquad (3)$$

where ξ_1 and ξ_2 are pressure loss coefficients. The first term of this second-order polynomial represents the pressure drop due to inertial effects (Forchheimer term), which dominates the pressure drop at high speeds, and the second term represent the pressure drop due to viscous effects (Darcy term) (Lage et al., 1997), which becomes important at low flow speeds.

3. Results and discussion

3.1 Cooling rate

3.1.1 Convective heat transfer coefficients

During forced-convective precooling, the cooling rate of the fruit is determined by the convective heat exchange at the fruit-air interface, which is usually quantified by means of convective heat transfer coefficients (CHTCs). In a related study (Defraeye et al., 2013), the magnitude of these CHTCs and their heterogeneity within a specific container and between individual containers was investigated for standard, Supervent and Ecopack containers. Only a single flow rate was evaluated for each container, namely 0.19, 0.65 and 2.12 L $s^{-1}kg^{-1}$ of fruit for standard, Supervent and Ecopack containers, respectively. As mentioned above, these flow rates are representative for industrial forced convective precooling (Brosnan and Sun, 2001). The flow rate differed for each container as it was related to a specific fan. The standard container showed very low CHTCs, a large spread within a single container and also a significant CHTC variation between individual containers. The Supervent container but especially the Ecopack container showed higher CHTCs, amongst others due to their higher flow rate, but also a more homogeneous distribution, both within each container and between individual containers. For more detailed information on these distributions, the reader is referred to Defraeye et al. (2013).

The present study provides additional insight since the CHTCs at the fruit surface can be correlated with the air speed. These CHTCs, resulting from steady-state CFD simulations at three flow rates (see section 2.2), were determined for each computational cell on the surface of the oranges. CHTCs were based on the initial fruit temperature (20°C) and the inlet air temperature (-0.5°C). As such, the resulting CHTCs are actually directly proportional to the heat flux at the wall ($q_{c,w}$). For each row of containers, a correlation of the surface-averaged CHTC over that row with the approach flow air speed (average speed at the inlet of the computational domain, see Table 2) was determined. Depending on the quality of the approximation (R^2 value), a linear or power-law correlation was chosen as most appropriate. These correlations are presented in

Table 3. In addition, the CHTCs are given as a function of the approach flow air speed in Figure 3 for each row of containers as well as for the entire layer of containers (bold lines), for the three container designs. The CHTC distribution over the surfaces of the oranges is shown in Figure 4 at an imposed pressure difference of 10000 Pa, 1000 Pa and 10 Pa for standard, Supervent and Ecopack containers, respectively, since then the flow rate was quite similar for all containers (see Table 2). Normalisation of these CHTCs is done with the surface-averaged CHTC over the entire layer of containers at this flow rate.

At a certain flow rate and for a certain row, the standard container seems to have the highest CHTC of all packages, closely followed by Supervent. The CHTCs of Ecopack are clearly lower. The higher CHTCs for the CFC's at the same flow rate are attributed to the occurrence of high velocities induced by the jets in the openings of the containers (see Figure 4). Even though these higher (surface-averaged) CHTCs seem to be more beneficial, these local higher cooling rates are actually not desired since they introduce higher cooling heterogeneity of fruit within a container. Note that for the Ecopack container, high CHTCs are obtained at the sides of the stacks of oranges (Figure 4), since the resistance to airflow is less here as flow actually bypasses the stack (see also section 3.1.2).

In general, good correlations of the CHTC with the air speed were obtained. Although a power-law correlation is common for forced-convective heat transfer of bluff bodies (e.g., Defraeye et al., 2012), a linear correlation, with non-zero intercept, was found more appropriate for the second and third row of the CFC's. However, since most of these linear correlations had a negative intercept, which is physically not justified as it implies negative CHTCs at zero air speed, the power-law correlations (with a lower R^2 value) were also reported in these cases. The power-law exponent is however also different for that typically found for forced-convective turbulent heat transfer, which is usually below one (e.g. Defraeye et al., 2010). One of the reasons for these anomalies in the correlations could be that the CHTCs here are influenced by the heating up of the air in the first row, by which a power-law correlation or using the upstream approach flow temperature to calculate the CHTC may be less justified.

Note that a container design which provides the fastest cooling rate is not necessarily the best for fruit quality as chilling injury can occur during cooling of citrus fruit, especially at low temperatures such as applied for cold sterilisation treatments. Hence container cooling performance analysis should preferably be combined with an evaluation of chilling injury. Preliminary chilling injury data for these three container designs were already reported by Defraeye et al. (2013). The standard container showed the most chilling injury here.

3.1.2 Influence of airflow rate

The impact of airflow rate on the fruit cooling rate was evaluated by imposing different pressure differences over the layer of containers. In precooling systems, the flow rate and pressure drop are however determined by the intersection of the system curve with the fan performance curve. This working point differs for each container design and is also very system specific. As such, it is usually not justified to compare the cooling rate of different containers at a same pressure drop nor at the same flow rate: comparison at the same pressure drop implies that the fan curve is horizontal (ΔP as a function of G_a); comparison at the same flow rate implies that the fan can be tuned for each container to obtain this flow rate. The latter could be unrealistic when the same precooling system is used for different containers; even if the fan flow rate can be adjusted (e.g., by varying the rpm), the pressure drop curves for the containers can be too different here to allow a single fan to produce the same flow rate (see section 3.2). Therefore, comparing the impact of flow rate on the cooling behaviour for different containers should preferably be done in conjunction with the CHTCs, which were discussed in section 3.1.1, or by using a specific ventilation system (i.e., a single fan) to evaluate all package designs. The latter was done for the three package designs (at one flow rate) in a previous study (Defraeye et al., 2013), but in a laboratory setup rather than in a commercial context.

The fruit temperatures in the centre of the oranges are given in Figure 5 as a function of time for all virtual sensors (in the centre of a single orange, located in the central part of the container, section 2.4), but averaged over a specific row (see Figure 2 for row numbering). Results of the three container designs at three different flow rates are shown. The corresponding HCT ($t_{1/2}$) and SECT ($t_{7/8}$) of each row, i.e. obtained from the profiles of Figure 5, are presented in Figure 6 as a function of flow rate and pressure drop.

All HCT and SECT curves show a decreasing slope towards higher flow rates. For a similar pressure drop, the fruit in the standard container cools much slower than in the other two containers (Figure 6), due to the much lower flow rate. For a similar flow rate however, the standard container only shows a slightly lower cooling rate and for the third row, the HCT of the standard container is even lower than that of the Supervent container. For a similar flow rate, the differences between containers agree well with the CHTC behaviour (section 3.1.1). Nevertheless, some differences exist since HCT and SECT were evaluated in a single orange in the centre of the container, whereas CHTCs were surface-averaged, thus including all oranges.

Of all containers, the Ecopack container shows the fastest cooling for a similar pressure drop, due to the high flow rate, but the lowest cooling rate at a similar flow rate, due to the rather low CHTCs (see section 3.1.1 and Figure 3). However, as mentioned above, an evaluation of container performance should also take into account the cooling system since they are closely intertwined and determine together the working point of the system, which will be different for each container design. In the (single) ventilation system used by Defraeye et al. (2013), the Ecopack showed the best performance, but this is not necessarily the case for other systems. Nevertheless, the Ecopack cools the stack of oranges for an individual container in the most uniform way, which is beneficial for fruit quality (see Defraeye et al., 2013). The Ecopack cooling performance could probably even be improved by closing the airflow short circuits, namely the open air spaces on either side of the container next to the plastic foil (see Figure 1), as they create to some extent a preferential airflow pathway around the fruit (Defraeye et al., 2013).

Finally, a spread in the cooling rate was identified between the individual containers in each of the two most downstream rows for the standard container in a related study with CFD (Defraeye et al., 2013). This spread was caused by blockage of several vent holes between row 2 and row 3 in the CFD model for horizontal flow, since the standard container was not designed to be palletised, i.e., placed with its long side against its short side. This blockage, predominantly of the two middle containers in the last row of the standard container, was also indicated by the lower CHTCs in these containers (Figure 4). In reality, some airflow will always pass via these vents, due to imperfect stacking, as seen experimentally, which leads to more rapid cooling with less heterogeneity between the containers in a certain row (results not shown, see Defraeye et al., 2013). Although the CFD model was thus rather idealised for this container, a model adjustment to allow airflow via the central vents in the last row was not pursued due to the arbitrariness of these changes. For Supervent and Ecopack, this spread was much more limited.

3.1.3 Influence of set temperature

In the future, more South-African citrus export markets are expected to request cold sterilisation treatment (cooling to ≈ -0.5°C). This reduced set temperature will lead to a decreased throughput for the currently installed cooling installations. Instead of adjusting or expanding the current cooling capacity, new container designs (Supervent and Ecopack) were developed, amongst others, to maintain throughput in a cost-effective way when switching to the cold sterilisation protocol. Hence a comparison was made between the cooling time (thus achievable throughput) of the standard container to 4°C (current situation) and that of the Supervent and Ecopack containers to -0.5°C (a possible future situation). The latter should preferably provide a cooling time (to -0.5°C) that is equal to, or faster than that of the standard container (to 4°C).

The HCT and SECT of each row of the standard container when cooling to 4°C were within 1% of the ones which were presented in Figure 6 for cooling this container to -0.5°C. This was expected to some extent since these dimensionless parameters are characteristics of the precooling process and should be in essence quite independent of the set temperature, particularly since the heat transport properties were taken independent of temperature in the simulations. Hence, in the simulations, the cooling behaviour (shape of cooling curves) is quasi independent of the set temperature, by which the conclusions on the cooling rate for the standard container for cooling to 4°C are similar to those of section 3.1.2, when cooling to -0.5°C. In practice however, these dimensionless parameters (HCT and SECT) are rarely the same for different set temperatures, and are usually higher if the set temperature is lower. The HCT and SECT for the standard package will thus most probably be higher when cooling to -0.5°C, by which the throughput will in practice be lower.

When comparing the results at a similar flow rate and especially at a similar pressure drop from the simulations, the new containers show a similar performance or an improvement in HCT and SECT when used for cold sterilisation treatment (-0.5°C), compared to standard containers with normal treatment (4°C). The same or a higher throughput can thus be achieved with the new containers, compared to the standard container, even when cooling to a lower set temperature. For a similar flow rate however, Ecopack performs slightly worse. In addition, the new designs also produce more uniform cooling of the individual fruit in the containers.

3.2 System energy consumption

3.2.1 Pressure loss curves

The pressure loss curves as a function of flow rate (Eq. (3)) for horizontal flow through the computational model of the containers (single layer for CFC's and two layers for Ecopack, all containing in total the same amount of fruit, see Figure 2) are given in Table 4 for all three containers, as determined from regression analysis, and they are also shown in Figure 7. Differences between the containers are pronounced, with a much lower aerodynamic resistance for the Ecopack container, due to its very high total open area in the airflow direction.

3.2.2 Influence of airflow rate

Using the method explained in section 2.5, the energy needed to produce airflow through the computational model (Figure 2) during precooling, until the SECT is reached, is shown in Figure 8 as a function of flow rate and pressure drop over the model. The two new container designs clearly show potential for reducing the operational cost, compared to the standard container, both due to a reduction of required ventilation system power as well as a reduced SECT (Figure 6). The Ecopack obviously performs best here at a specific flow rate. These findings should however be combined with an integral system design to find the optimal airflow rate for a specific container design as many other parameters also play a role (see de Castro et al., 2005). In addition, the actual reduction of the operational costs due to a lower aerodynamic resistance of the containers will strongly depend on the resistances of the other components in the system as well.

3.2.3 Influence of set temperature

Since the SECT for the standard container, cooled to 4°C was very similar to that cooled to -0.5°C, Figure 8 is also representative for the system energy needed to cool to 4°C and the same conclusions hold. However, cold sterilisation treatment (to -0.5°C) requires more field heat to be removed which will increase the energy consumption of the cooling system compared to the normal treatment. This difference in field heat to be removed can be easily estimated based on the heat capacity, the density and the temperature difference between initial fruit temperature (20°C) and set temperature (-0.5°C or 4°C). Cooling down to -0.5°C required 28% more energy, compared to 4°C (relative to 4°C).

4. Conclusions

The influence of cooling conditions for orange fruit precooling (airflow rate, cooling temperature) on the cooling rate and system energy consumption was evaluated for three package designs within the context of cold sterilisation treatments for the South-African citrus industry. Both an existing standard container as well as two new container designs, namely Supervent and Ecopack, were evaluated, stacked on a pallet, by means of computational fluid dynamics (CFD).

With respect to cooling, Ecopack showed a lower convective heat transfer rate than the other two containers, for the same flow rate through the containers. Ecopack, however, cooled the oranges in the most uniform way, which is beneficial for fruit quality. The higher cooling rate of standard and Supervent was attributed to the high-velocity jets in the (circular) openings in the containers. The convective heat transfer coefficients at the surfaces of the oranges correlated well with the air speed, where linear or power-law correlations were found to provide a good approximation. Furthermore, the seven-eighths cooling time (SECT) of fruit cooled to normal temperatures for orange precooling (≈ 4°C) was very similar to that found for cold sterilisation treatment (≈ -0.5°C). As such, the new package designs provide similar or even better cooling behaviour for cold sterilisation than the standard package under normal conditions.

With respect to the energy needed to maintain airflow through the pallet of containers during precooling until the SECT is reached, the new designs used less energy due to their lower aerodynamic resistance and lower cooling time, particularly the Ecopack. In conclusion, these new containers seem a cost-effective way for maintaining or even increasing throughput when switching to cold sterilisation treatment. In addition, they also reduce the energy load on the system and provide more uniform cooling of the oranges in the containers.

Note however that apart from the pressure loss characteristics of the containers, the aerodynamic resistances in the rest of the system and the fan curve are also critical determinants of the working point of the system, thus of the resulting flow rate through the pallets of containers. Since this working point is very case- and system-specific, it is often not straightforward to compare cooling rates and cooling performances of different containers designs, as they should in principle be assessed together with the specific cooling system which is used. This study however mainly aimed at providing basic information for preliminary design decisions or for altering existing cooling protocols or cooling systems. In a next step, this knowledge and the developed computational models will be used to optimise such protocols or systems more in detail, with respect to cooling time and homogeneity, throughput, fruit quality and operational cost of the system.

Acknowledgements

Thijs Defraeye is a postdoctoral fellow of the Research Foundation – Flanders (FWO) and acknowledges its support. Financial support by the Research Foundation – Flanders (project FWO G.A108.10) is gratefully acknowledged. This work is based upon research supported by the South African Research Chairs Initiative of the Department of Science and Technology and the National Research Foundation. The contribution of the Department of Science and Technology through the South African Post-Harvest Innovation Programme (project “Packaging of the Future”) is also acknowledged. We would like to acknowledge Cedarpack packhouse, Dr. Graham Barry from XLnT Citrus which supplied the Ecopack containers and Dawid Groenewald from the Citrus Research International Postharvest Technical Forum for logistical and technical support with this study.

Defraeye T., Lambrecht R., Delele M.A., Ambaw A., Opara U.L., Cronjé P., Verboven P., Nicolai B. (2014), Forced-convective cooling of citrus fruit: cooling conditions and energy consumption in relation to package design, *Journal of Food Engineering* 121, 118-127. http://dx.doi.org/10.1016/j.jfoodeng.2013.08.021

References

Ambaw, A., Verboven, P., Delele, M.A., Defraeye, T., Tijskens, E., Shenk, A., & Nicolai, B. (2012). CFD modelling of the 3D spatial and temporal distribution of 1-methylcyclopropene in a fruit storage container. *Food and Bioprocess Technology* (DOI:10.1007/s11947-012-0913-7).

ASHRAE (1994). *ASHRAE Handbook - Refrigeration: systems and applications* (SI edition). ASHRAE, Atlanta, USA.

ASHRAE (1993). *ASHRAE Handbook - Fundamentals* (SI edition). ASHRAE, Atlanta, USA.

Brosnan, T., & Sun, D.-W. (2001). Precooling techniques and applications for horticultural products - a review. *International Journal of Refrigeration*, 24(2), 154-170.

de Castro, L.R., Vigneault, C., & Cortez, L.A.B. (2005). Effect of container openings and airflow rate on energy required for forced-air cooling of horticultural produce. *Canadian Biosystems Engineering*, 47, 1-9.

Defraeye, T., Blocken, B., & Carmeliet, J. (2010). CFD analysis of convective heat transfer at the surfaces of a cube immersed in a turbulent boundary layer. *International Journal of Heat and Mass Transfer*, 53(1-3), 297-308.

Defraeye, T., Lambrecht, R., Ambaw, A., Delele, M.A., Opara, U.L., Cronjé, P., Verboven, P., & Nicolai, B. (2013). Forced-convective cooling of citrus fruit: package design. *Journal of Food Engineering*, In press (doi:10.1016/j.jfoodeng.2013.03.026).

Defraeye, T., Herremans, E., Verboven, P., Carmeliet, J., & Nicolai, B. (2012). Convective heat and mass exchange at surfaces of horticultural products: a microscale CFD modelling approach. *Agricultural and Forest Meteorology*, 162-163, 71-84.

Dehghannya, J., Ngadi, M., & Vigneault, C. (2010). Mathematical modeling procedures for airflow, heat and mass transfer during forced convection cooling of produce: a review. *Food Engineering Reviews*, 2 (4), 227-243.

Dehghannya, J., Ngadi, M., & Vigneault, C. (2011). Mathematical modeling of airflow and heat transfer during forced convection cooling of produce considering various package vent areas. *Food Control*, 22(8), 1393-1399.

Dehghannya, J., Ngadi, M., & Vigneault, C. (2012). Transport phenomena modelling during produce cooling for optimal package design: Thermal sensitivity analysis. *Biosystems Engineering*, 111(3), 315-324.

Delele, M., Tijskens, E., Atalay, Y.T., Ho, Q.T., Ramon, H., Nicolai, B., & Verboven, P. (2008). Combined discrete element and CFD modelling of airflow through random stacking of horticultural products in vented boxes. *Journal of Food Engineering*, 89(1), 33-41.

Delele, M.A., Ngcobo, M.E.K., Opara, U.L., & Meyer, C.J. (2012). Investigating the effects of table grape package components and stacking on airflow, heat and mass transfer using 3-D CFD modelling. *Food and Bioprocess Technology* (DOI:10.1007/s11947-012-0895-5).

Delele, M.A., Schenk, A., Tijskens, E., Ramon, H., Nicolai, B.M., & Verboven, P. (2009). Optimization of the humidification of cold stores by pressurized water atomizers based on a multiscale CFD model. *Journal of Food Engineering*, 91(2), 228-239.

FAO (2009). Food and Agriculture Organisation of the United Nations - Global agriculture towards 2050. Available at: www.fao.org/fileadmin/templates/wsfs/docs/Issues_papers/HLEF2050_Global_Agriculture.pdf. Accessed 23 February 2012.

FAOSTAT (2012). Food and Agriculture Organisation of the United Nations. Available at: http://faostat.fao.org. Accessed on 23 February 2012.

Ferrua, M.J., & Singh, R.P. (2009). Design guidelines for the forced-air cooling process of strawberries. *International Journal of Refrigeration*, 32(8), 1932-1943.

Franke, J., Hellsten, A., Schlünzen, H., & Carissimo, B. (2007). Best practice guideline for the CFD simulation of flows in the urban environment. COST Action 732: Quality assurance and improvement of microscale meteorological models, Hamburg, Germany.

Gowda, B.S., Narasimham, G.S.V.L., & Murthy, M.V.K. (1997). Forced-air precooling of spherical foods in bulk: A parametric study. *International Journal of Heat and Fluid Flow*, 18(6), 613-624.

Hu, Z., & Sun, D.-W. (2001). Predicting the local surface heat transfer coefficients by different turbulent k-ε models to simulate heat and moisture transfer during air-blast chilling. *International Journal of Refrigeration*, 24(7), 702-717.

Kondjoyan, A. (2006). A review on surface heat and mass transfer coefficients during air chilling and storage of food products. *International Journal of Refrigeration*, 29(6), 863-875.

Lage, J.L., Antohe, B.V., & Nield, D.A. (1997). Two types of nonlinear pressure-drop versus flow-rate relation observed for saturated porous media. *Journal of Fluids Engineering*, 119(3), 700-706.

Menter, F.R., 1994. Two-equation eddy-viscosity turbulence models for engineering applications. AIAA Journal 32 (8), 1598-1605.

Nahor, H., Hoang, M., Verboven, P., Baelmans, M., & Nicolai, B. (2005). CFD model of the airflow, heat and mass transfer in cool stores. *International Journal of Refrigeration*, 28(3), 368-380.

Pathare, P.B., Opara, U.L., Vigneault, C., Delele, M.A., & Al-Said, F.A. (2012). Design of packaging vents for cooling fresh horticultural produce. *Food and Bioprocess Technology*, 5(6), 2031-2045.

Roache, P.J. (1994). Perspective: a method for uniform reporting of grid refinement studies. *Transactions of the ASME - Journal of Fluids Engineering*, 116(3), 405-413.

Smale, N.J., Moureh, J., & Cortella, G. (2006). A review of numerical models of airflow in refrigerated food applications. *International Journal of Refrigeration*, 29(6), 911-930.

Thompson, A.K. (2003). *Fruit and Vegetables - Harvesting, Handling and Storage* (1st ed.). Blackwell Publishing Ltd., Oxford, UK.

van der Sman, R.G.M. (2002). Prediction of airflow through a vented box by the Darcy–Forchheimer equation. *Journal of Food Engineering*, 55(1), 49-57.

Verboven, P., Datta, A.K., Anh, N.T., Scheerlinck, N., & Nicolai, B. (2003). Computation of airflow effects on heat and mass transfer in a microwave oven. *Journal of Food Engineering*, 59(2-3), 181-190.

Verboven, P., Flick, D., Nicolai, B., & Alvarez, G. (2006). Modelling transport phenomena in refrigerated food bulks, packages and stacks: basics and advances. *International Journal of Refrigeration*, 29(6), 985-997.

Zou, Q., Opara, L.U., & McKibbin, R. (2006a). A CFD modeling system for airflow and heat transfer in ventilated packaging for fresh foods I: Initial analysis and development of mathematical models. *Journal of Food Engineering*, 77(4), 1037-1047.

Defraeye T., Lambrecht R., Delele M.A., Ambaw A., Opara U.L., Cronjé P., Verboven P., Nicolai B. (2014), Forced-convective cooling of citrus fruit: cooling conditions and energy consumption in relation to package design, *Journal of Food Engineering* 121, 118-127. http://dx.doi.org/10.1016/j.jfoodeng.2013.08.021

Zou, Q., Opara, L.U., & McKibbin, R. (2006b). A CFD modeling system for airflow and heat transfer in ventilated packaging for fresh foods II: Computational solution, software development and model testing. *Journal of Food Engineering*, 77(4), 1048-1058.

Tables

Table 1. Total open area of standard, Supervent and Ecopack containers.

	Short side	Long side
Standard	2.0%	1.5%
Supervent	3.1%	3.5%
Ecopack	not relevant	57.9%

Table 2. Flow rate, average air speed at inlet of computational domain and average superficial air speed inside the fruit stacks for three container designs at different pressure differences over the layer of containers.

	Superficial speed (m s^{-1})				Average speed at inlet (m s^{-1})				Flow rate (L $s^{-1}kg^{-1}$ of fruit)			
	10 Pa	100 Pa	1000 Pa	10000 Pa	10 Pa	100 Pa	1000 Pa	10000 Pa	10 Pa	100 Pa	1000 Pa	10000 Pa
Standard	-	0.10	0.32	1.03	-	0.04	0.13	0.40	-	0.08	0.25	0.79
Supervent	-	0.37	1.17	3.71	-	0.14	0.46	1.45	-	0.28	0.90	2.85
Ecopack	0.84	2.80	9.07	-	0.35	1.15	3.73	-	0.85	2.81	9.10	-

Table 3. Parameters *a* and *b* in linear and power-law correlations of the CHTC with the air speed at the inlet of the computational domain (U, m s^{-1}): CHTC = $aU+b$ (lin.) or = aU^b (pow.) ([a]: although a linear correlation gave a better correlation coefficient, a negative intercept *b* was present, and therefore a power law correlation is also reported here).

	Standard				Supervent				Ecopack			
	Type	a	b	R^2	Type	a	b	R^2	Type	a	b	R^2
Total	Lin.	27.5	0.13	1.000	Pow.	21.7	0.91	0.999	Pow.	17.1	0.71	1.000
Row 1	Pow.	39.5	0.78	1.000	Pow.	32.1	0.71	1.000	Pow.	20.1	0.63	1.000
Row 2	Lin. [a]	28.6	-0.64	1.000	Lin.	20.9	0.43	0.998	Pow.	14.0	0.83	0.998
	Pow.	39.2	1.32	0.993								

Defraeye T., Lambrecht R., Delele M.A., Ambaw A., Opara U.L., Cronjé P., Verboven P., Nicolai B. (2014), Forced-convective cooling of citrus fruit: cooling conditions and energy consumption in relation to package design, *Journal of Food Engineering* 121, 118-127. http://dx.doi.org/10.1016/j.jfoodeng.2013.08.021

Row 3	Lin. [a]	14.65	-0.66	0.995	Lin. [a]	14.99	-1.19	1.000	-	-	-	-
	Pow.	30.6	1.78	0.989	Pow.	13.6	1.32	0.993				

Table 4. Pressure loss curves (polynomial approximations) for the computational model (single layer of containers for CFC's and two layers for Ecopack) as a function of the flow rate through the computational domain (G_a in m³ s^{-1}) for three container designs.

Container design	Polynomial approximation
Standard	$\Delta P = 5.94 \times 10^5 G_a^2 + 11.5 G_a$
Supervent	$\Delta P = 4.52 \times 10^4 G_a^2 + 62.0 G_a$
Ecopack	$\Delta P = 4.35 \times 10^2 G_a^2 + 14.3 G_a$

Figure captions

Figure 1. Geometry and dimensions of the standard and Supervent corrugated fibreboard containers and the Ecopack reusable plastic container.

Figure 2. Computational model and boundary conditions for standard (similar to Supervent) and Ecopack containers.

Figure 3. Surface-average convective heat transfer coefficient (CHTC) for each row of containers as a function of average air speed (at inlet of domain) for the three container designs. The bold lines (total) indicate the average value over the entire layer of containers.

Figure 4. Distribution of CHTCs over surfaces of oranges for three different container designs at a specific pressure difference (different for each container). The CHTCs are normalised with the surface-averaged CHTC over all oranges and all containers.

Figure 5. Temperatures in the centre of the oranges in each row of containers (averaged over all virtual sensors in the row, *y*-direction, row 1 is the upstream row) for the standard, Supervent and Ecopack containers for three flow rates (indicated by pressure differences), as a function of time.

Figure 6. HCT ($t_{1/2}$) and SECT ($t_{7/8}$) for each row of containers (averaged over all virtual sensors in the oranges in the row, *y*-direction, row 1 is the upstream row) for the standard (ST), Supervent (SV) and Ecopack (EP) containers for three flow rates, as a function of both pressure difference and flow rate (logarithmic scale).

Figure 7. Pressure loss over the computational model (Figure 2) as a function of the flow rate through the computational domain for three container designs. The data points (dots) as well as the second-order polynomial approximations (Poly.) are shown.

Figure 8. Energy required to maintain airflow through the computational model (Figure 2) until the SECT is reached for different container designs (logarithmic scale), as a function of airflow rate.

Defraeye T., Lambrecht R., Delele M.A., Ambaw A., Opara U.L., Cronjé P., Verboven P., Nicolai B. (2014), Forced-convective cooling of citrus fruit: cooling conditions and energy consumption in relation to package design, *Journal of Food Engineering* 121, 118-127. http://dx.doi.org/10.1016/j.jfoodeng.2013.08.021

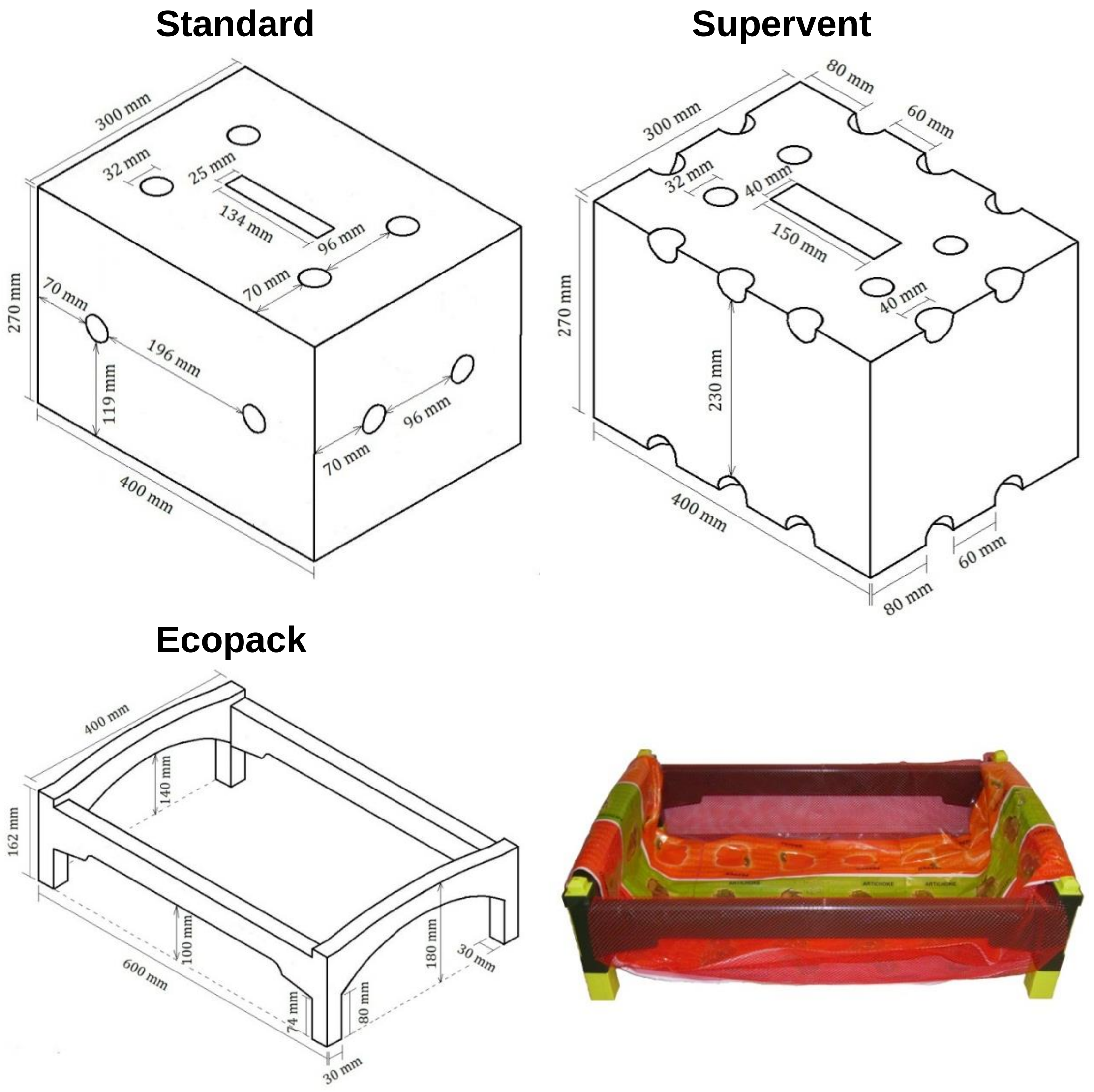

Figure 1. Geometry and dimensions of the standard and Supervent corrugated fibreboard containers and the Ecopack reusable plastic container.

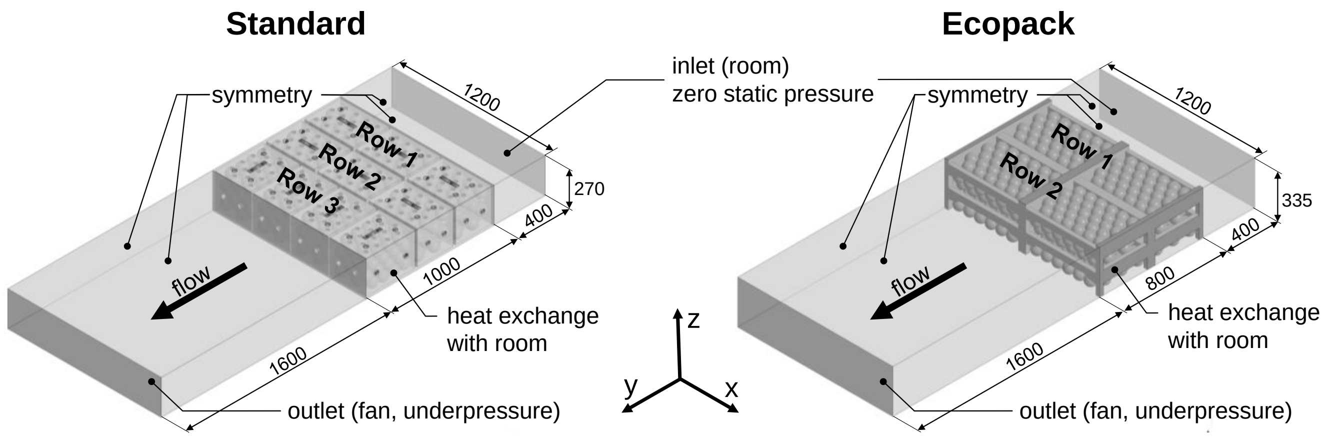

638

639 Figure 2. Computational model and boundary conditions for standard (similar to Supervent) and Ecopack

640 containers.

641

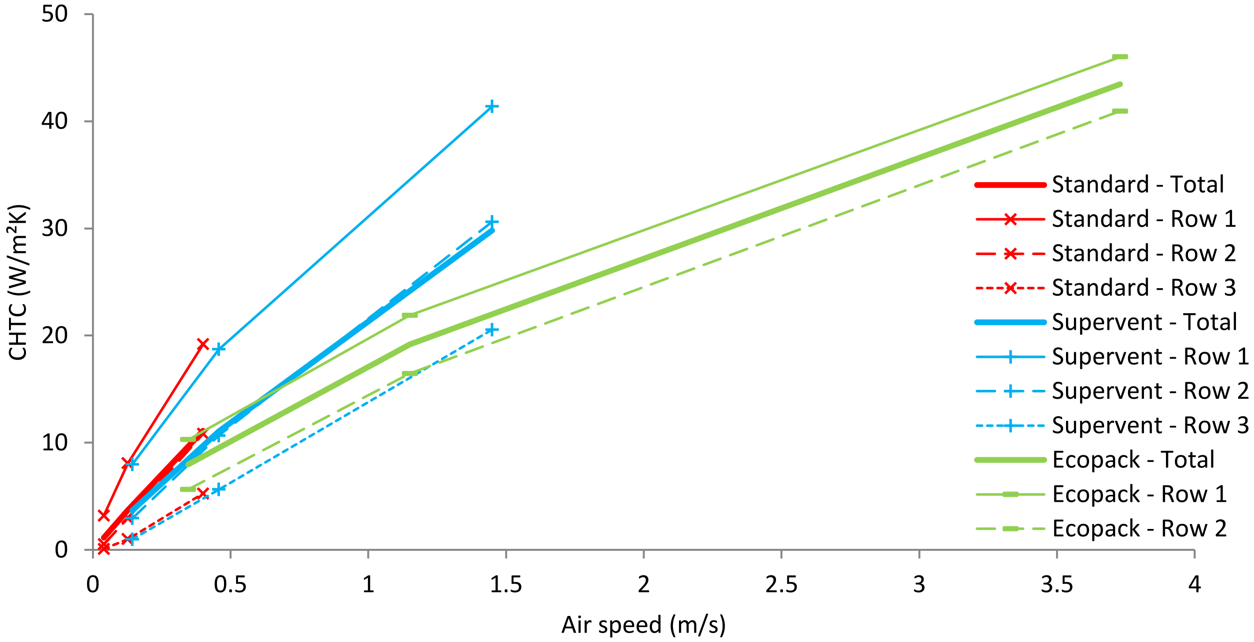

Figure 3. Surface-average convective heat transfer coefficient (CHTC) for each row of containers as a function of average air speed (at inlet of domain) for the three container designs. The bold lines (total) indicate the average value over the entire layer of containers.

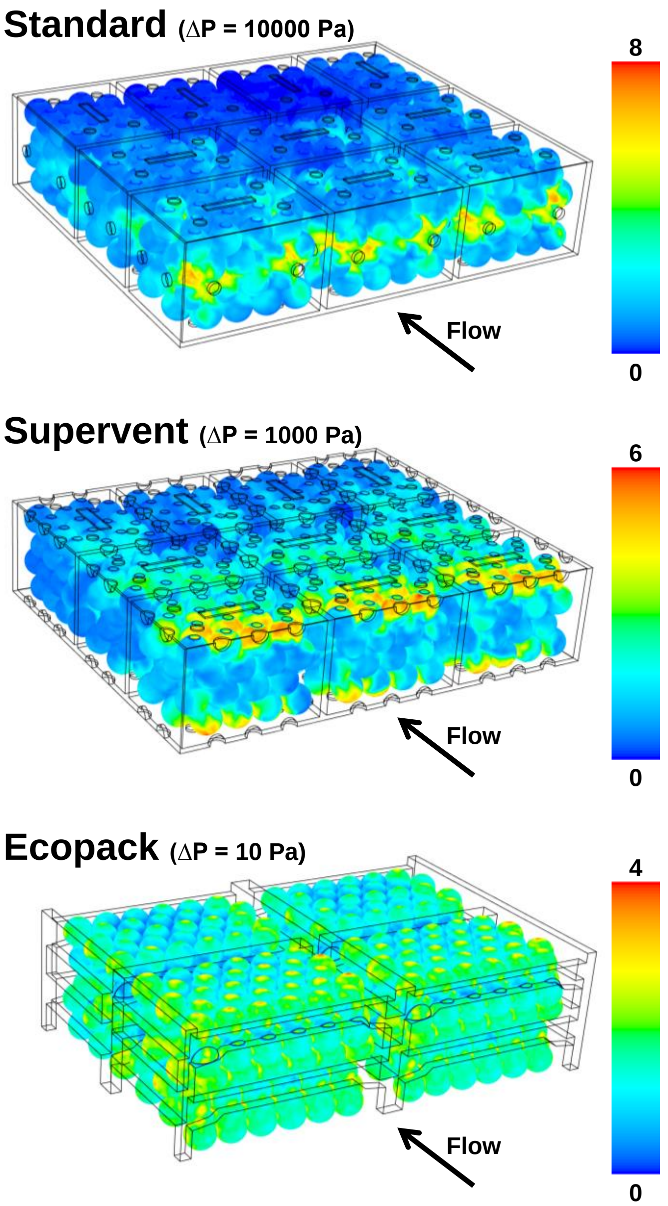

Figure 4. Distribution of CHTCs over surfaces of oranges for three different container designs at a specific pressure difference (different for each container). The CHTCs are normalised with the surface-averaged CHTC over all oranges and all containers.

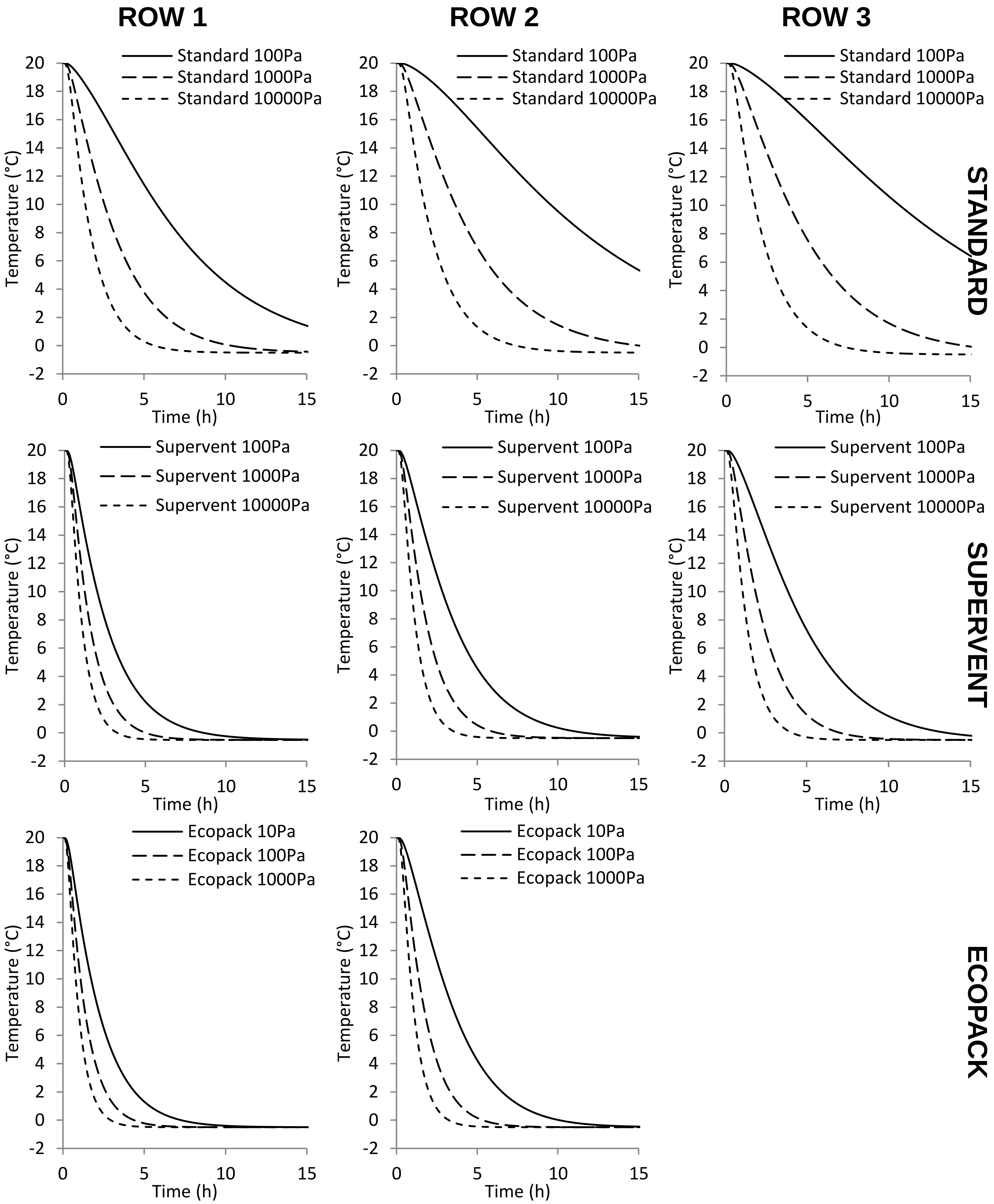
ROW 1
ROW 2
ROW 3
STANDARD
SUPERVENT
ECOPACK
Standard 100Pa
Standard 1000Pa
Standard 10000Pa
Supervent 100Pa
Supervent 1000Pa
Supervent 10000Pa
Ecopack 10Pa
Ecopack 100Pa
Ecopack 1000Pa
Temperature (°C)
Time (h)

Figure 5. Temperatures in the centre of the oranges in each row of containers (averaged over all virtual sensors in the row, *y*-direction, row 1 is the upstream row) for the standard, Supervent and Ecopack containers for three flow rates (indicated by pressure differences), as a function of time.

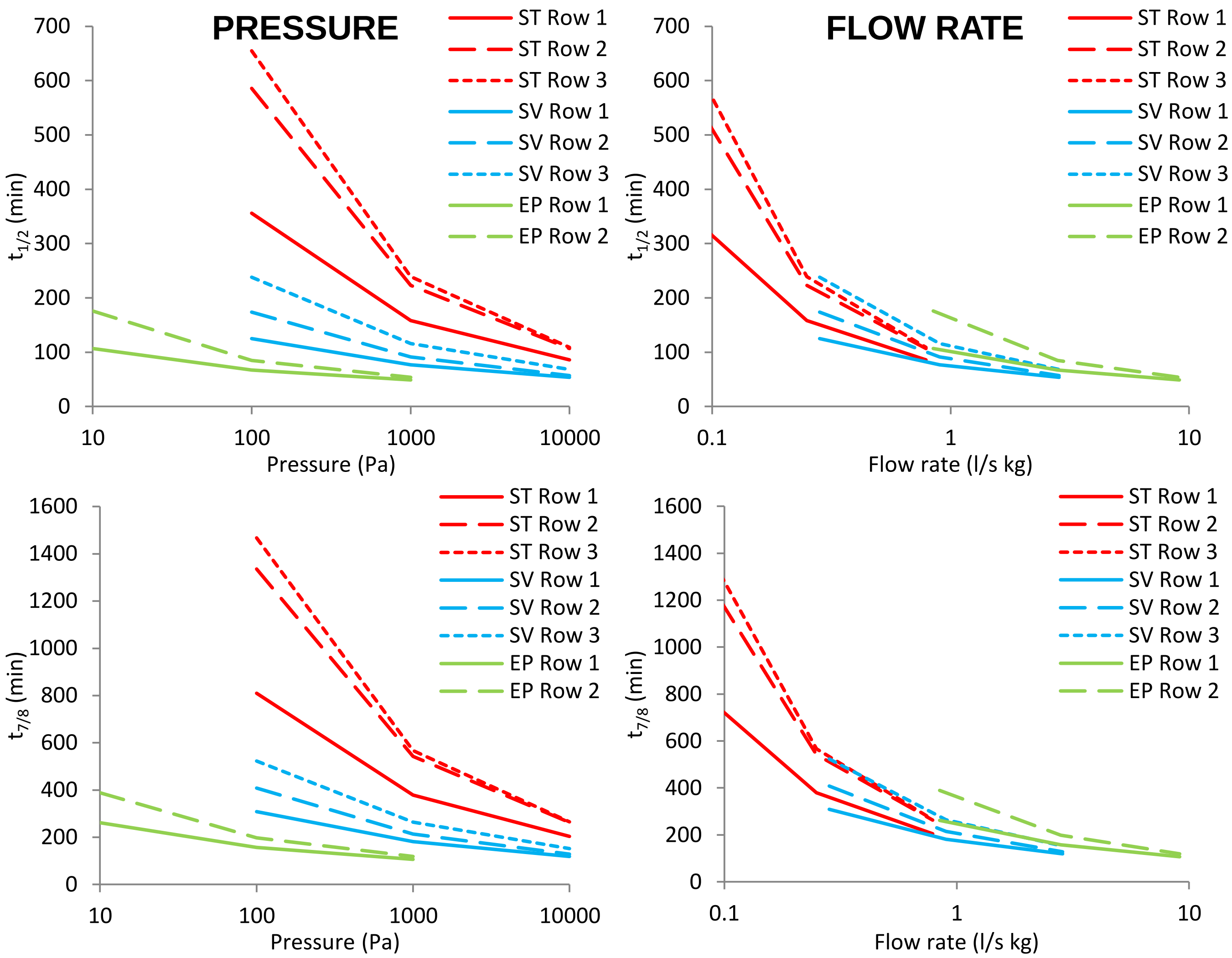

Figure 6. HCT ($t_{1/2}$) and SECT ($t_{7/8}$) for each row of containers (averaged over all virtual sensors in the oranges in the row, *y*-direction, row 1 is the upstream row) for the standard (ST), Supervent (SV) and Ecopack (EP) containers for three flow rates, as a function of both pressure difference and flow rate (logarithmic scale).

Defraeye T., Lambrecht R., Delele M.A., Ambaw A., Opara U.L., Cronjé P., Verboven P., Nicolai B. (2014), Forced-convective cooling of citrus fruit: cooling conditions and energy consumption in relation to package design, *Journal of Food Engineering* 121, 118-127. http://dx.doi.org/10.1016/j.jfoodeng.2013.08.021

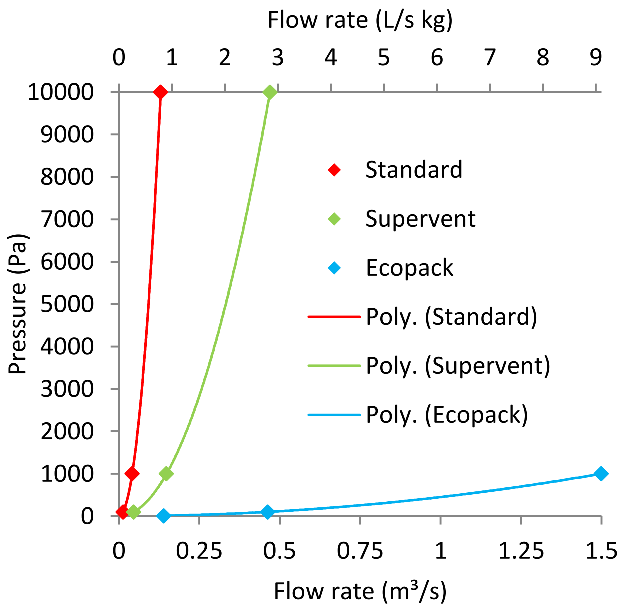

Figure 7. Pressure loss over the computational model (Figure 2) as a function of the flow rate through the computational domain for three container designs. The data points (dots) as well as the second-order polynomial approximations (Poly.) are shown.

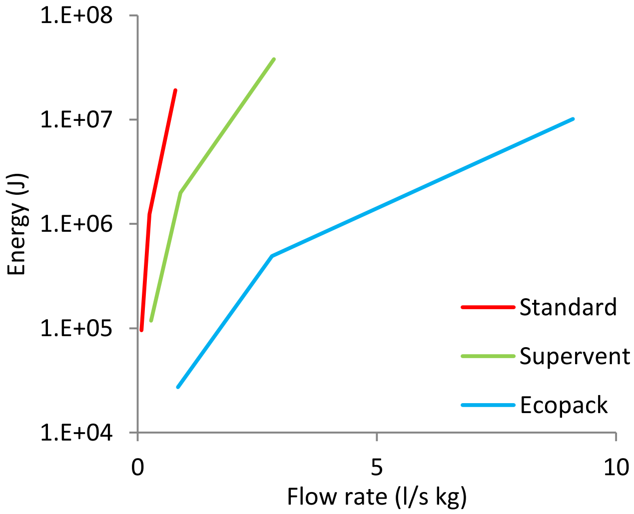

Figure 8. Energy required to maintain airflow through the computational model (Figure 2) until the SECT is reached for different container designs (logarithmic scale), as a function of airflow rate.